

1
2
3
4
5
6
7
8
9
10
11
12
13
14
15
16
17
18
19
20
21

The importance of CH₄ ebullition in floodplain fens

K. M. Stanley^{1,2}, C. M. Heppell¹, L. R. Belyea¹, A. J. Baird³ and R.H. Field⁴

¹ School of Geography, Queen Mary University of London, London, UK.

² Current address: Atmospheric Chemistry Research Group, School of Chemistry, University of Bristol, Bristol, UK.

³ School of Geography, University of Leeds, Leeds, UK.

⁴ RSPB Centre for Conservation Science, Royal Society for the Protection of Birds, Sandy, UK.

Corresponding author: Catherine Heppell (c.m.heppell@qmul.ac.uk)

Key Points:

- CH₄ ebullition flux shows more temporal than spatial variability in two reed-dominated floodplain fens
- CH₄ ebullition flux can exceed diffusive and plant-mediated fluxes in spring and early summer
- CH₄ ebullition flux increases with soil temperature and water level, and decreases with increasing plant cover

22 Abstract

23 Uncertainty in estimates of CH₄ emissions from peatlands arise, in part, due to difficulties in
24 quantifying the importance of ebullition. This is a particular concern in temperate lowland
25 floodplain fens in which total CH₄ emissions to the atmosphere (often measured as the sum of
26 diffusive and plant-mediated fluxes) are known to be high, but few direct measurements of
27 CH₄ ebullition fluxes have been made. Our study quantified CH₄ fluxes (diffusion, plant-
28 mediated and ebullition) from two temperate floodplain fens under conservation management
29 (Norfolk, UK) over 176 days using funnels and static chambers. CH₄ ebullition was a major
30 component (> 38 %) of total CH₄ emissions over spring and summer. Seasonal variations in
31 quantifiable CH₄ ebullition fluxes were marked, covering six orders of magnitude (5×10^{-5} to
32 $62 \text{ mg CH}_4 \text{ m}^{-2} \text{ h}^{-1}$). This seasonal variability in CH₄ ebullition fluxes arose from changes in
33 both bubble volume flux and bubble CH₄ concentration, highlighting the importance of
34 regular measurements of the latter for accurate assessment of CH₄ ebullition using funnels.
35 Soil temperature was the primary control on CH₄ ebullition fluxes. Elevated water level was
36 also associated with increased CH₄ ebullition fluxes, with a distinct increase in CH₄ ebullition
37 flux when water level rose to within 10 cm of the peat surface. In contrast, CH₄ ebullition
38 flux decreased steadily with increasing plant cover (measured as Vascular Green Area).
39 Ebullition was both steady and episodic in nature; and drops in air pressure during the two-
40 day funnel deployments were associated with higher fluxes.

41

42 1 Introduction

43 The contemporary global warming or cooling effect of peatlands is influenced
44 disproportionately by emissions of the potent but short-lived greenhouse gas, CH₄ (Frolking
45 & Roulet, 2007), leading to concern about the potential for peatland management to
46 unintentionally increase CH₄ emissions and exacerbate radiative forcing (Abdalla et al., 2016;
47 Petrescu et al., 2015). Estimates of peatland CH₄ emissions are uncertain (Limpens et al.,
48 2008), in part because of difficulties in quantifying reliably the contribution from one of the
49 main CH₄ transport mechanisms, ebullition or bubbling (Baird et al., 2009; Ramirez et al.,
50 2017; Yu et al., 2014). Ebullition may be steady or episodic (Goodrich et al., 2011). Green
51 and Baird (2012) define the former as a steady stream of CH₄-containing bubbles released to
52 the water table, and note that it is analogous to the steady release of bubbles (albeit ones
53 containing CO₂) seen in vats of fermenting beer. Green and Baird (2012) also note that
54 bubbles may be released in short-lived (minutes to hours) bursts, with fluxes during these
55 bursts being much higher and more variable than background steady fluxes. They term such

56 bursts episodic ebullition. The amount of CH₄ transported to the water table via ebullition
57 depends on both bubble volume flux and CH₄ concentration (Coulthard et al., 2009).
58 Measurements using funnel traps show high spatiotemporal heterogeneity in bubble volume
59 flux (Baird et al., 2004; Green & Baird, 2012, 2013; Stamp et al., 2013). Upscaling (Bon et
60 al., 2014; Coulthard et al., 2009) and managing (Abdalla et al., 2016; Petrescu et al., 2015)
61 CH₄ effluxes will require greater understanding of the spatial and temporal factors controlling
62 both components of ebullition: bubble volume flux and CH₄ concentration.

63
64 Temperature, water level, and microbial substrate availability are widely-recognized as the
65 key controls on ecosystem-scale CH₄ emissions (e.g., Bubier et al., 1993; Christensen et al.,
66 2003). Ebullition depends on these factors, as well as on sub-surface peat properties that
67 affect the growth, storage and release of gas bubbles (Yu et al., 2014). High rates of ebullition
68 (> ~10 mg CH₄ m⁻² hr⁻¹) can be triggered by episodic events such as gusts of wind, drops in
69 hydrostatic pressure or changes in barometric pressure (Coulthard et al., 2009; Kellner et al.,
70 2006; Strack et al., 2005, Goodrich et al., 2011), but rapid CH₄ transport can also occur
71 through plants (Shannon et al., 1996; Noyce et al., 2014). Besides providing a direct,
72 competing mechanism for rapid transport of CH₄, emergent macrophytes affect CH₄
73 ebullition indirectly (Chanton, 2005; Laanbroek, 2010) by (i) producing labile carbon, which
74 becomes substrate for methanogens and (ii) supplying oxygen to the rhizosphere, which fuels
75 CH₄ oxidation as well as the recycling of alternative terminal electron acceptors involved in
76 competing redox processes.

77
78 Although the contribution of ebullition to total CH₄ emission from bogs has been quantified
79 in a few studies (Baird et al., 2004; Chen & Slater, 2015; Stamp et al., 2013), the importance
80 of ebullition as a component of CH₄ emissions from floodplain fens has not yet been
81 characterized. Total CH₄ effluxes from temperate floodplain fens are reported as an order of
82 magnitude greater than from ombrotrophic bogs (Audet et al., 2013; Hendriks et al., 2007),
83 even though the fen measurements omitted ebullition fluxes. The dominance of emergent
84 macrophytes, as well as persistently high water levels, may help explain why CH₄ emissions
85 are particularly high from groundwater-fed peatlands, or fens (Turetsky et al., 2014). A recent
86 analysis highlighted the potentially large - but highly uncertain - extent of peat-forming
87 riparian wetlands, including floodplain fens dominated by emergent macrophytes (Gumbrecht
88 et al., 2017). Ebullition fluxes from these systems are likely to be strongly influenced by
89 management of vegetation and water levels (Abdalla et al., 2016). Furthermore, given the
90 similarities in vegetation type between temperate and tropical floodplain fens, and with

91 *Phragmites australis* (Cav.) Trin. ex Steud. being the most abundant wetland species globally
92 (van den Berg et al., 2016), findings from research carried out on reed-dominated temperate
93 floodplain fen sites may also be applicable to other regions.

94
95 Our research aimed to quantify CH₄ fluxes at two temperate floodplain fen sites under
96 conservation management, using a combination of static chambers and funnel traps to
97 establish the importance of ebullition as a CH₄ transport pathway. Specific research questions
98 were as follows:

99
100 RQ1. How variable are CH₄ ebullition fluxes over the growing season and across reed-
101 dominated sites of contrasting productivity?

102
103 RQ2. Which environmental factors control CH₄ ebullition flux and its components (CH₄
104 concentration, bubble volume flux)?

105
106 RQ3. What is the overall importance of CH₄ ebullition flux as a proportion of total CH₄ flux
107 to the atmosphere over the growing season at the two sites?

108 **2 Study sites**

109 The study took place at two lowland floodplain fens: Sutton (1°30'E 52°45'N) and
110 Strumpshaw Fen (1°27'E 52°36'N), in the Norfolk Broads, UK (Figure 1) from 13th March to
111 5th September 2013. Fens cover the largest area of any lowland peatland type in England and
112 Wales (Natural England, 2010) and are widely distributed throughout northern temperate
113 zones (Cadillo-Quiroz et al., 2008; Turetsky et al., 2014). In the UK it is estimated that fen,
114 reedbed, lowland raised bog and grazing marsh together cover at least 392,000 ha, of which
115 fen covers 140,000 ha (Maltby et al., 2011; Baird et al., 2009), but the exact extent of
116 floodplain fen is uncertain. Both sites are dominated by *P. australis* (Table 1) which is
117 globally widespread and abundant, occurring in many wetland habitats (IUCN, 2017). In the
118 UK, fens are valued for their high biodiversity (UK Biodiversity Action Plan, 2008), and as
119 locations of significant carbon storage (Baird et al., 2009). Although the two sites are reed-
120 dominated, they have contrasting nutrient status. The relatively high nutrient (N and P)
121 content of both peat and vegetation at Strumpshaw in relation to Sutton Fen (Table 1) enabled
122 characterization of CH₄ fluxes across the range of nutrient status found in floodplain fens in
123 agricultural landscapes in Europe, based on foliar (Boorman & Fuller, 1981; Olde Venterink
124 et al., 2001) and soil nutrient contents (Syed et al., 2006; Wassen & Olde Venterink, 2006)
125 reported in the literature. Hereafter, we refer to Strumpshaw Fen as NB-HN (Norfolk Broads-

126 High Nutrient) and Sutton Fen as NB-LN (Norfolk Broads-Low Nutrient). The codes here are
127 also used by the Defra-funded Project SP1210 ‘Lowland Peatland Systems in England and
128 Wales’ of which these sites were a component. The two sites are both deep peat fens under
129 conservation management which aims to maintain floral diversity to benefit invertebrate and
130 bird habitat. Vegetation is cut on a rotation to prevent succession into fen carr and to reduce
131 dominance by tall plant species. Reeds at both sites had previously been cut four years prior
132 to the study. Water levels at NB-HN are controlled by embankments between the fen and its
133 adjacent river, whilst at NB-LN there are no embankments next to the river. A network of
134 sluices and ditches are used at both sites to control the flow of water around the fens, and to
135 ensure high water tables throughout most of the year.

136

137 **3 Methods**

138 3.1 Overall approach and environmental variables

139 CH₄ fluxes were measured from 13 March 2013 (Day of Year 72) to 5 September 2013 (Day
140 of Year 248) using six static chambers and 12 inverted glass funnels at each site (described in
141 Sections 3.2 and 3.3; Figure S1). The chamber measurements captured CH₄ fluxes by
142 diffusion, plant-mediated transport and steady ebullition. The funnel measurements captured
143 CH₄ fluxes by steady and episodic ebullition. Thus, in this study, steady ebullition fluxes
144 were measured by both chambers and funnels, and the implications of this for interpretation
145 of the importance of ebullition as a contributor to total CH₄ fluxes are discussed in Sections
146 3.5 and 5.3.

147

148 Measurements were taken within a 0.04 km² area at each site where the vegetation had been
149 harvested in 2009, ensuring that *P. australis* was at a comparable stage of growth in both
150 sites. An automatic weather station (MiniMet, Skye Instruments, UK) at each site provided
151 hourly averages of air temperature, soil temperature at 5 cm depth, net radiation, air pressure,
152 wind speed and direction, and hourly rainfall totals. Water level was measured hourly using
153 pressure transducers in dipwells at six locations adjacent to chamber collars (Levellogger
154 Gold, Solinst, Canada). Seasonal variability in plant biomass within chamber collars was
155 monitored non-destructively following each measurement of CH₄ flux using an allometric
156 technique that quantifies vascular green area (VGA; Wilson et al., 2007). Peat stratigraphy of
157 15 × 3 m cores collected systematically from each site was described using the von Post
158 measure of humification and a simplified Troels-Smith system for peat composition (Shotyk,
159 1988; Troels-Smith, 1955). A detailed description of the vegetation at each site can be found

160 in Table S1, and a description of the depth-distribution of peat composition at each site is
161 provided in Table S2.

162 3.2 Steady and episodic CH₄ ebullition fluxes measured using funnels

163 Time-integrated measurements of combined steady and episodic CH₄ ebullition flux were
164 taken using the inverted funnel method outlined in Stamp et al. (2013). Glass funnels had a
165 diameter of 0.2 m and 3 mm thick walls to eliminate gas permeation losses (Figure S2a). The
166 funnel spouts were replaced by 0.1 m cylindrical glass tubing, with an internal diameter of
167 0.036 m and 3 mm thick walls. A rubber bung was used at the top of the cylinder to form a
168 seal, and each bung was drilled and fitted with a syringe sampling tube (Tygon, 3.2 mm
169 internal diameter) terminating in a three-way valve. The funnels were wrapped in a silvered
170 cover to minimize solar heating, except for a north-facing strip of glass fitted with a
171 graduated scale to enable reading of the water level in the funnel. The inverted funnels were
172 inserted into shallow pits cut into the peat surface to a depth of 0.4 m to ensure the base of the
173 funnel was permanently below the water table and left in situ for the entire field campaign
174 (Figure S2b). Funnels were tall enough that when located in the shallow pit, the top
175 cylindrical portion of the funnel was above the peat surface and the graduated scale could be
176 read from a short distance. When in position, each funnel was filled with water, which was
177 displaced by rising bubbles. A volumetric rate of ebullition, here termed bubble volume flux,
178 was estimated by reading the level of the gas-water interface in the funnel. The concentration
179 of CH₄ within the trapped bubbles was quantified by extracting the trapped bubble headspace
180 for measurement. The removal of the trapped bubbles also allowed the funnel to be re-set for
181 the next measurement period.

182

183 CH₄ ebullition flux was quantified using 12 funnels at each site; however, one funnel broke at
184 NB-HN in March 2013, leaving 11 at that site. A total of 132 measurements were made over
185 the field campaign. Each month, all funnels were visited and sampled over a two-day period.
186 Each funnel was filled with water on day one and the bubble volume was recorded 48 hours
187 later, and bubble gas samples were taken for analysis. Funnels were sampled between 09:00
188 and 17:00 GMT (local time) by firstly recording the bubble volume to ± 2 mm from a
189 distance of 2 m using binoculars to prevent observer-induced ebullition. A 15 mL gas sample
190 was then extracted using a syringe and injected into a 12 mL pre-evacuated exetainer (Labco
191 Limited, Ceredigion, Wales). For gas samples < 15 mL, the gas headspace from the funnel
192 along with the required amount of water to make up 15 mL of sample was taken. The Bunsen
193 coefficient was used to account for CH₄ in the aqueous phase (Yamamoto et al., 1976).

194 Atmospheric temperature and pressure were also noted at the time of sampling using a
195 thermo-hygro-barometer (Commeter C4141, Czech Republic). The gas samples were
196 analyzed for CH₄ content using a gas chromatograph coupled with a flame ionization detector
197 as outlined in Baird et al. (2010). Hourly steady fluxes and averaged rates of ebullition from
198 the funnels were calculated following the method described in Stamp et al. (2013).

199 3.3 Diffusive, plant mediated and steady ebullition fluxes of CH₄ measured by static chamber

200 Steady fluxes, a combination of diffusive, plant-mediated and steady ebullition, were
201 measured using a transparent, segmented, 1.5-m tall, static chamber fitted to a collar (Figure
202 S3a). Six collars (60 cm × 60 cm × 20 cm – width × length × depth; Figure S3b) were
203 inserted to a depth of 18 cm at each site. The basal area and volume of the chambers were
204 0.36 m² and 0.54 m³, respectively. The vegetation was not cut to fit the size of the chamber
205 because this can alter gas exchange rates. Temperature, humidity and barometric pressure
206 were measured during chamber deployment using a Commeter C4141. A pressure
207 equalization balloon, ice packs and four fans were used to keep conditions within the
208 chamber similar to those outside the chamber. A 1.5 m length of Tygon tubing (3.2 mm i.d.)
209 was used for headspace sampling (Hornibrook et al., 2009) so that observer-induced effects
210 on CH₄ flux caused by standing next to the chamber were minimized.

211
212 Static chamber measurements of CH₄ flux were taken every month between 09:00 and 17:00
213 (GMT). Headspace samples of 15 mL were taken using a syringe and transferred to a pre-
214 evacuated exetainer (Labco Limited, Ceredigion, Wales) via a three-way valve. Headspace
215 samples were then extracted every two minutes for 20 minutes, and every 10 minutes
216 thereafter for 60 minutes. The gas samples were analyzed for CH₄ content using a gas
217 chromatograph coupled with a flame ionization detector as outlined in Baird et al. (2010).

218
219 CH₄ fluxes arising from linear increases in CH₄ concentrations in chambers were calculated
220 using linear regression and were based on the equations in Denmead (2008) and method
221 described in Stamp et al. (2013). A LINEST array function in Excel was used to test the
222 goodness of fit. The threshold used to accept the flux calculation was $R^2 > 0.9$. None of the
223 chamber measurements yielded non-linear chamber responses, interpreted as caused by
224 episodic ebullition events (Altor & Mitsch, 2006). Linear increases in CH₄ concentration in
225 chambers arise from a combination of three transport pathways: diffusion, plant-mediated and
226 steady ebullition (Hoffmann et al., 2017).

227

228 3.5 Statistical analysis

229 Generalized additive mixed models (GAMMs; Lin and Zhang, 1999) were fitted to the funnel
230 measurements of bubble volume flux, CH₄ concentrations, and CH₄ ebullition flux (i) to
231 quantify spatial and temporal variability (RQ1) and (ii) to assess relationships with
232 controlling environmental factors (RQ2). A GAMM quantifying spatial and temporal
233 variability was also fitted to the static chamber measurements of CH₄ flux to facilitate
234 comparison of time-integrated chamber and funnel fluxes (RQ3). GAMMs were chosen
235 because these models are easily interpreted and clearly encode the contribution of different
236 predictor variables, but they are more flexible than their linear counterparts because the
237 relationships between the dependent and independent variables may be non-linear. Including
238 both fixed and random effects was important in this study because samples were collected
239 from the same funnels over time, and hence observations from the same funnel may be
240 correlated.

241

242 All models were fitted using the gam function in R (R Core Team, 2017) from the gamm4
243 package (Wood & Scheipl, 2017), specifying a log-linked gamma distribution and a
244 continuous autoregressive structure (corCAR1) to account for temporal autocorrelation of
245 residuals for individual funnels. For analysis of temporal and spatial variability, day of year
246 was included as a smooth term to account for seasonality, site (NB-HN or NB-LN) was
247 included as a fixed factor on the intercept, and replicate funnels within each site were treated
248 as random effects on the intercept. For analysis of controlling factors, we initially considered
249 several environmental variables as potential predictors; a Pearson correlation matrix showed
250 that many of these variables were correlated with one another, so we fit models using only a
251 subset. For this subset, we chose mean soil temperature and mean water level, commonly
252 used in many other studies, as indicators of conditions relevant to CH₄ production and
253 oxidation; the standard deviation and slope of air pressure (calculated over the previous 48-
254 hrs, corresponding to the duration of funnel deployment) as indicators of conditions relevant
255 to ebullition; and VGA (mean of six collars measured concurrently with chamber flux) as an
256 indicator of vascular plant phenology. Models were fit using each of these predictors, as well
257 as their combination, and the corrected Akaike Information Criterion (AICc) was used to
258 select the most parsimonious model. During model selection, maximum likelihood (ML) was
259 used as the estimation method, whereas restricted maximum likelihood (REML) was used to
260 obtain final model fits.

261

262 In order to quantify the overall importance of CH₄ ebullition flux as a proportion of total flux
263 to the atmosphere (RQ3), we used both chamber and funnel measurements to separate CH₄
264 fluxes over the season into contributions from two different sets of transport mechanisms:
265 diffusion + plant-mediated transport (D + P) versus steady + episodic ebullition (S + E).
266 Since steady ebullition may be included in both chamber (D + P + S) and funnel (S + E)
267 measurements, it is impossible to partition the fluxes unequivocally. Instead, we constrained
268 our estimates by formulating two idealized extreme models (Zeide, 1991). First, if steady
269 ebullition is zero (S = 0), the funnel captures episodic ebullition (E) only; total emission is
270 equal to the sum of chamber and funnel fluxes (D + P + E) and (D + P) is equal to chamber
271 flux. Second, if episodic ebullition is zero (E = 0), the funnel captures steady ebullition only;
272 total emission is equal to chamber flux only (D + P + S) and (D + P) is equal to chamber
273 minus funnel flux. Since chamber and funnel fluxes were unpaired, we used the time-series
274 GAMMs to predict daily chamber and funnel fluxes for each replicate and then computed
275 mean chamber and funnel fluxes for each site for each day. We then back-transformed these
276 mean fluxes to original units, and calculated (D + P) and (S + E) contributions under the two
277 extreme models for each day. Both extreme models ignore bubble production in the 40-cm
278 thick zone above the funnels, and they both assume that bubbles collected by the funnels at
279 40 cm depth would have been transported to the peatland surface without oxidation. When
280 integrating flux contributions over the growing season, we assumed that bubbles released
281 CH₄ to the atmosphere only when the water table was within 5 cm of the peat surface; when
282 water tables were more than 5 cm below the surface, we made the conservative assumption
283 that CH₄ in bubbles was completely oxidized before reaching the atmosphere, and hence that
284 the (S + E) ebullition contribution to total CH₄ flux was zero.

285 **4 Results**

286 4.1 Spatial and temporal variations in CH₄ ebullition fluxes.

287 The time-series models (i.e., using day of year as the predictor; Table 2; Figure 2; Table S3)
288 explained more than 60% of the deviance in bubble volume flux (62 % of deviance
289 explained), CH₄ concentration in bubbles (68 %) and CH₄ ebullition flux (73 %). All three
290 response variables varied by several orders of magnitude over the season (Figure 2): bubble
291 volume flux and CH₄ ebullition flux both peaked in May and June, whereas CH₄
292 concentration in bubbles remained near-constant during this time. Both CH₄ concentration
293 and CH₄ ebullition flux decreased in August corresponding to a period of drying and a
294 marked drop in water table at both sites (Figure S4b). These seasonal patterns contrast

295 markedly with the relatively stable CH₄ fluxes from the static chambers (Figure 2d; 66 % of
296 deviance explained).

297

298 Along with these marked seasonal patterns, bubble volume flux, CH₄ concentration in
299 bubbles and CH₄ ebullition flux also showed some spatial differences. CH₄ concentration in
300 bubbles varied significantly amongst funnels within sites (Table S3) and, across sites, was
301 significantly higher at NB-LN than at NB-HN ($F_{1,94} = 12.7, p = 0.00058$). In contrast, bubble
302 volume and CH₄ ebullition fluxes showed little fine-scale variation amongst funnels within
303 sites (Table S3; Figure S5b) and showed only small and non-significant (5 % significance
304 level) differences between sites (bubble volume flux: $F_{1,99} = 3.23, p = 0.071$; CH₄ ebullition
305 flux: $F_{1,98} = 3.19, p = 0.078$). When integrated over the season using the time-series
306 GAMMs, these small but consistent between-site differences resulted in CH₄ ebullition fluxes
307 that were two-fold higher at NB-LN than at NB-HN (Figure 4a).

308

309 Overall, our data show that CH₄ ebullition flux varies much more strongly over the season
310 than across microsites, and the reason for this temporal variation is the focus of our modelling
311 effort described in Section 4.2.

312

313 4.2 Factors controlling temporal variations in CH₄ ebullition.

314 The environmental models (i.e., using the most parsimonious combination of environmental
315 factors as predictors; Table 3) accounted for over two-thirds of the deviance in bubble
316 volume flux (66 % of deviance explained), CH₄ concentration (74 %) and CH₄ ebullition flux
317 (73 %), whereas the fixed effect of site was redundant in all final models (Table 3). These
318 models highlight the importance of water level, VGA and soil temperature on CH₄
319 concentration and CH₄ ebullition flux. Mean water levels more than 10 cm below ground
320 surface were associated with very low CH₄ concentrations and CH₄ ebullition fluxes (Figure
321 3). CH₄ concentration and CH₄ ebullition flux decreased steadily with increasing VGA. The
322 three response variables showed contrasting relationships with mean soil temperature: bubble
323 volume flux reached its peak at intermediate soil temperatures (10-12 °C), CH₄ concentration
324 remained low and then increased markedly at temperatures above 10 °C, and CH₄ ebullition
325 flux increased almost log-linearly with temperature across the observed range. Finally, whilst
326 air pressure was not a significant factor controlling CH₄ concentration, there was a weak
327 negative relationship between variability in air pressure and bubble volume flux whilst a drop
328 in air pressure during funnel deployment was associated with higher CH₄ ebullition fluxes.

329 Random variation amongst funnels was significant for CH₄ concentration, but not for bubble
330 volume or CH₄ ebullition flux (Table S4), indicating that some fine-scale spatial controls on
331 CH₄ concentration were not captured by our field campaign.

332 4.3 The overall importance of CH₄ flux via ebullition.

333 Chamber and funnel methods yielded seasonal CH₄ fluxes of similar magnitude. Seasonal
334 chamber flux was comparable at NB-LN and NB-HN, whereas seasonal funnel flux was two-
335 fold larger at NB-LN (Figure 4a). Contrasting estimates were obtained for the contributions
336 from different transport pathways across the two extreme models (Figure 4b). Under the first
337 extreme model (assuming steady ebullition = 0), a large percentage of total CH₄ flux
338 integrated over the season was contributed by episodic ebullition: 38 % for NB-HN and 54 %
339 for NB-LN. Recall that we have made the conservative assumption that ebullition did not
340 contribute to total CH₄ flux at all when water levels dropped more than 5 cm below the
341 peatland surface. When integrated only over the periods of high water levels, the contribution
342 of episodic ebullition to total CH₄ flux was even greater (54 % for NB-HN and 81 % for NB-
343 LN). Funnel fluxes exceeded chamber fluxes for a large part of the growing season. Hence
344 the second extreme model (assuming episodic ebullition = 0) yielded negative contributions
345 for diffusive + plant-mediated fluxes (Figure 4b). This implausible result indicates either net
346 uptake of CH₄ from atmosphere to soil or, more likely, that the assumption of zero episodic
347 ebullition was unfounded.

348 **5 Discussion and Conclusions**

349 5.1 Spatial and temporal variation in CH₄ ebullition in temperate floodplain fens.

350 CH₄ ebullition fluxes from the funnel traps varied seasonally by six orders of magnitude,
351 whereas CH₄ fluxes from the static chambers showed less variation. The strong, seasonal
352 patterns in ebullition, contrary to previous studies from *P. australis*-dominated wetlands
353 (Flury et al., 2010), was partly due to a sharp late-season drop in bubble CH₄ concentration,
354 but it was driven mainly by changes in bubble volume flux which depends on the inter-
355 relations among the rise velocity, number and size of bubbles released. The volume of
356 bubbles captured by the funnels was associated with changes in air pressure, suggesting the
357 contribution of a physical mechanism triggering bubble release.

358

359 Bubble CH₄ concentration is sometimes measured less frequently by researchers than bubble
360 volume flux (Comas & Wright, 2012), but our study shows that an accurate assessment of

361 CH₄ ebullition flux in floodplain fens requires repeated measurements of CH₄ bubble
362 concentrations over the season. The consistent, significant difference in CH₄ concentration in
363 bubbles between our two sites could be explained by edaphic factors such as substrate
364 composition, and/or differences in peat nutrient status, through an influence on both plant
365 productivity and biogeochemical cycling. The contrasting nutrient status of our two sites has
366 resulted in greater plant productivity at NB-HN compared to NB-LN, as exemplified by a
367 significant difference in above-ground biomass (Table 1). The higher plant productivity at
368 NB-HN may result in enhanced CH₄ oxidation at depths > 40 cm in the peat (the depth of the
369 funnels) compared with NB-LN, due to greater radial oxygen loss around plant roots
370 (Armstrong & Armstrong, 1991; Armstrong et al., 1996).

371

372 Spatial variability in CH₄ ebullition flux in these *P. australis*-dominated fens was low, in
373 contrast with the fine-scale hot-spots of ebullition activity observed in *Sphagnum* spp.-
374 dominated northern peatlands and in the Florida Everglades (Comas & Wright, 2012; Stamp
375 et al., 2013). Whilst Stamp et al. (2013) noted a 500-fold difference (0.016 – 7.515 g CH₄ m⁻²)
376 in the highest and lowest summed CH₄ ebullition fluxes measured using funnel traps within
377 a single raised bog, our floodplain fen data for a similar time frame show only a three-fold
378 difference (5 – 15 g CH₄ mg m⁻²) in summed fluxes, across two sites of contrasting nutrient
379 status, suggesting that upscaling of ebullition fluxes can be more confidently performed with
380 fewer replicates in floodplain fens than in raised bogs (Ramirez et al., 2017). This has
381 important cost-saving implications for field studies designed for the purpose of upscaling to
382 regional or landscape scales, and for constructing greenhouse gas budgets.

383 5.2 Environmental factors controlling temporal variations in CH₄ ebullition

384 Soil temperature exerted strong control on CH₄ ebullition, with 10 °C marking a threshold
385 above which CH₄ concentration increased rapidly, whereas bubble volume flux switched
386 from a positive to a negative temperature-dependence. Temperature causes increases in both
387 microbial production and consumption of CH₄ up to about 20 to 25 °C (Kotsyurbenko et al.,
388 2004), but the temperature-dependence of microbial production outstrips that of consumption
389 (van Winden et al., 2012). Besides promoting greater microbial activity, increasing
390 temperature increases bubble volume (Fechner-Levy & Hemond, 1996) and reduces gas
391 solubility in water (Clever & Young, 1987). At temperatures below 10 °C, temperature-
392 induced increases in gas-phase CH₄ were accommodated by an increase in bubble volume
393 flux, through either larger and faster-rising bubbles (cf. Smirnov and Berry, 2015) or a

394 greater number of bubbles, or a combination of both (Figure 3a). At higher temperatures,
395 increases in gas-phase CH₄ were accommodated by an increase in bubble CH₄ concentration,
396 despite a concomitant decrease in bubble volume flux. These competing temperature-driven
397 processes led to a near-constant log-linear increase in CH₄ ebullition flux across the observed
398 temperature range (Figure 3f).

399 Bubble CH₄ concentration and CH₄ ebullition flux decreased with increasing VGA,
400 highlighting the role of vascular plants as a control on ebullition, albeit one that was
401 secondary to temperature. The interplay between ebullition, plant-mediated transport and
402 rhizospheric oxidation is not yet fully understood (Green & Baird, 2012). Some researchers
403 have suggested that vascular plants may reduce CH₄ concentration in pore waters (and thus
404 bubbles) by transporting CH₄ to the atmosphere and simultaneously transferring oxygen to
405 their roots (Chanton, 2005; Strack et al., 2017). However, vascular plants could also increase
406 dissolved CH₄ concentrations because their root exudates act as a source of labile carbon,
407 promoting CH₄ production (Green & Baird, 2012; Joabsson & Christensen, 2001).
408 Throughout our entire field campaign NB-HN had overall higher VGA, and also lower CH₄
409 concentration in bubbles, in comparison to NB-LN (Figure S4d and Figure 2). Hence, our
410 results suggest that the net effect of increasing vascular plant biomass at floodplain fen sites
411 is a decrease in CH₄ concentration and also CH₄ ebullition fluxes (Figure 3).

412 The importance of water level as a control on CH₄ concentration and ebullition flux is also
413 highlighted by this research, and appears to take the form of a threshold effect. An enlarged
414 unsaturated zone increases the potential for CH₄ oxidation in peat and diminishes CH₄
415 production (Hornibrook et al., 2009). The net effect of these processes is to decrease the
416 concentration of dissolved CH₄ in the unsaturated zone, usually to c. 0 μmol L⁻¹. Low
417 concentrations of CH₄ can also occur below the water table, and the depth at which such low
418 concentrations persist varies by peatland, and with rainfall duration and magnitude
419 (Hornibrook et al., 2009). At NB-LN and NB-HN, CH₄ concentrations in bubbles collected at
420 40 cm depth decreased markedly when the water table dropped 20 – 25 cm below the peat
421 surface, during a period of very low rainfall (c. 30 mm over 6 weeks). This might indicate
422 that oxygen is penetrating over 15 cm below the water table (via diffusion or rhizospheric
423 oxidation), consequently elevating CH₄ oxidation rates relative to production at 40 cm, and
424 thus lowering CH₄ concentrations in bubbles that are trapped by the funnels.

425 5.3 The overall significance of ebullition fluxes in lowland floodplain fens

426 We have measured amongst the highest ebullition fluxes recorded to date in peatlands (up to
427 $1490 \text{ mg CH}_4 \text{ m}^{-2} \text{ d}^{-1}$; compared with fluxes in Table 1 of Yu et al. (2014)) and shown that
428 ebullition contributes over 38 % of spring and summer CH_4 emissions from these floodplain
429 fens. Our findings confirm that ebullition is a significant transport mechanism for CH_4 release
430 from peatlands (Coulthard et al., 2009), even in fens dominated by vascular plants that
431 transport CH_4 from the soil to the atmosphere. During periods when water levels remained
432 within 5 cm of the peat surface, ebullition was the dominant contributor to CH_4 emissions.
433 The increases in bubble volume and CH_4 ebullition fluxes that occurred with changes in air
434 pressure, as well as the large excess of funnel fluxes (sum of episodic + steady ebullition
435 fluxes) over chamber fluxes (sum of diffusive + plant-mediated + steady ebullition fluxes)
436 during periods of high water levels, point to episodic release being a major component of
437 CH_4 ebullition flux. Sampling programs that fail to capture episodic ebullition could badly
438 under-estimate total CH_4 emissions from these landscapes.

439 The implications of ebullition for total CH_4 emission will depend on how much, if any, CH_4
440 is stripped from bubbles as they move from the depth of ebullition flux measurement (in this
441 case 40 cm depth) to the atmosphere. CH_4 fluxes measured by the funnels exceeded those
442 from chamber measurements at a time when the water table was above the soil surface (> 5
443 cm) at NB-HN and within 5 cm of the surface at NB-LN, when the saturated zone is likely to
444 be predominantly anoxic. However, the extent of CH_4 oxidation as the bubbles move towards
445 the water-air interface is likely to differ across sites, and will depend on rates of CH_4
446 oxidation versus bubble residence time. To our knowledge, no studies have directly measured
447 CH_4 oxidation rates in floodplain fens and it is an area warranting further study.

448

449 Does it matter whether CH_4 -containing bubbles are released steadily or episodically? In order
450 to quantify adequately the episodic component of ebullition, researchers need to know when
451 to target field measurements. Episodic ebullition can be triggered by abrupt rises and falls in
452 barometric pressure (Comas & Wright, 2012; Glaser et al., 2004; Strack et al., 2005; Tokida
453 et al., 2005) or water level, but considerable uncertainty remains regarding the relative
454 importance of each (Chen & Slater, 2015). We found that atmospheric pressure drops were
455 associated with higher ebullition fluxes than atmospheric pressure increases, whilst rises or
456 falls in water level were not a significant controlling factor. The greatest atmospheric
457 pressure drop (measured as the overall slope of 48-hrs' data) that we recorded during funnel
458 deployment was 50 Pa h^{-1} which is comparable to the magnitude of pressure drops found by
459 Tokida et al. (2005) to cause episodic ebullition from a bog peat monolith. In our study, the

460 drops in air pressure occurred with the passage of cold fronts across the UK from the
461 Atlantic. Pressure changes arising from the passage of low pressure weather systems could
462 give rise to significant increases in CH₄ ebullition fluxes from lowland peatlands, with
463 episodic ebullition events superimposed over steady ebullition fluxes. Automated gas traps
464 and chambers (Goodrich et al., 2011; Comas & Wright, 2012; Hoffmann et al., 2017) provide
465 the high temporal resolution sampling required to separate CH₄ contributions from steady and
466 episodic ebullition. As discussed above, this approach needs to be combined with repeated
467 measurement of CH₄ concentration.

468

469 Management of water levels and vegetation in floodplain fens has the potential to alter the
470 relative importance of different CH₄ transport mechanisms, and hence the total CH₄ flux to
471 the atmosphere. By their very nature, floodplain fens are associated with rapid increases in
472 water level, which Bon et al. (2014) suggest can trigger significant ebullition events. We did
473 not measure ebullition during two large rainfall events in winter 2013, when increases in river
474 level at both sites led to flooding of the order of tens of centimetres. Future research should
475 aim to assess the influence of such events on the magnitude of episodic ebullition from
476 floodplain fens, as well as the impact of artificially maintaining high water levels. Vegetation
477 management practices such as reed-cutting, which reduce vascular plant biomass for several
478 years, have the potential to reduce plant-mediated transport of CH₄ but also to increase CH₄
479 ebullition by limiting the magnitude of rhizospheric CH₄ oxidation. Further investigation is
480 warranted on the net effect of these common management practices on total CH₄ emissions.

481 5.4 Conclusions

482 Ebullition is a major component (> 38%) of CH₄ emissions from temperate floodplain fens
483 over spring and summer, showing considerable temporal variation arising from changes in
484 water level, plant phenology and air pressure. Significant challenges remain in quantifying
485 the importance of different CH₄ transport pathways; however, such apportionment of
486 transport mechanisms is necessary to understand the effect of management strategies on
487 reducing CH₄ emissions from lowland fens. Specifically, total CH₄ emissions will depend on
488 how CH₄ ebullition and plant-mediated CH₄ transport respond to management of both water
489 level and vegetation.

490 **Acknowledgments and Data**

491 All authors designed the study; AJB, CMH, KMS and LRB co-designed the chambers and
 492 funnels; AJB and Sophie Green (University of Exeter) designed and supplied the spreadsheet
 493 to convert field data into fluxes; KMS carried out the field and laboratory work; LRB and
 494 CMH analyzed the data and wrote the paper; all authors edited the text. The research was
 495 funded by a UK Natural Environment Research Council (NERC) studentship (NEC04526)
 496 and a Queen Mary University of London studentship (both awarded to KMS), and by the UK
 497 Government's Department for Environment, Food and Rural Affairs (Defra) (contract
 498 SP1210, awarded to CMH). Project data is available to download from NERC EIDC: see
 499 links provided in Heppell et al., 2018). We thank the Royal Society for the Protection of
 500 Birds and their reserve managers, Tim Strudwick and Richard Mason, for allowing access to
 501 the research sites and for their logistical help. Andrew Skinner (RSPB) is thanked for the
 502 vegetation surveys, and Kate Peel for help with fieldwork and laboratory analyses. We would
 503 also like to thank the Associate Editor, Patrick M Crill, and two anonymous reviewers for
 504 their constructive and helpful comments on the manuscript.

505 References

- 506 Abdalla, M., Hastings, A., Truu, J., Espenberg, M., Mander, Ü., & Smith, P. (2016). Emissions of methane from
 507 northern peatlands: a review of management impacts and implications for future management options. *Ecology*
 508 *and Evolution*, 6(19), 7080-7102. doi:10.1002/ece3.2469
- 509 Altor, A. E., & Mitsch, W. J. (2006). Methane flux from created riparian marshes: Relationship to intermittent
 510 versus continuous inundation and emergent macrophytes. *Ecological Engineering*, 28(3), 224-234.
 511 doi:10.1016/j.ecoleng.2006.06.006
- 512 Armstrong, J., & Armstrong, W. (1991). A convective through-flow of gases in *Phragmites australis* (Cav.)
 513 Trin. ex Steud. *Aquatic Botany*, 39(1), 75-88. doi:10.1016/0304-3770(91)90023-X
- 514 Armstrong, J., Armstrong, W., Beckett, P., Halder, J., Lythe, S., Holt, R., & Sinclair, A. (1996). Pathways of
 515 aeration and the mechanisms and beneficial effects of humidity- and Venturi-induced convections in *Phragmites*
 516 *australis* (Cav.) Trin. ex Steud. *Aquatic Botany*, 54(2), 177-197.
- 517 Audet, J., Johansen, J. R., Andersen, P. M., Baattrup-Pedersen, A., Brask-Jensen, K. M., Elsgaard, L.,
 518 Kjaergaard, C., Larsen, S. E., & Hoffmann, C. C. (2013). Methane emissions in Danish riparian wetlands:
 519 Ecosystem comparison and pursuit of vegetation indexes as predictive tools. *Ecological Indicators*, 34(0), 548-
 520 559. doi:10.1016/j.ecolind.2013.06.016
- 521 Baird, A. J., Beckwith, C. W., Waldron, S., & Waddington, J. M. (2004). Ebullition of methane-containing gas
 522 bubbles from near-surface Sphagnum peat. *Geophysical Research Letters*, 31(21). doi:10.1029/2004GL021157
- 523 Baird, A.J., Holden, J. & Chapman, P. (2009) A Literature Review of Evidence on Emissions of Methane in
 524 Peatlands, Defra Project SP0574, 54 pp.
- 525 Baird, A. J., Comas, X., Slater, L. D., Belyea, L. R., & Reeve, A. S. (2009). Understanding Carbon Cycling in
 526 Northern Peatlands: Recent Developments and Future Prospects. *Carbon Cycling in Northern Peatlands*.
 527 Washington, DC: American Geophysical Union.
- 528 Baird, A. J., Stamp, I., Heppell, C. M., & Green, S. M. (2010). CH₄ flux from peatlands: a new measurement
 529 method. *Ecohydrology*, 3(3), 360-367. doi:10.1002/Eco.109
- 530 Bon, C. E., Reeve, A. S., Slater, L., & Comas, X. (2014). Using hydrologic measurements to investigate free-
 531 phase gas ebullition in a Maine peatland, USA. *Hydrol. Earth Syst. Sci.*, 18(3), 953-965. doi:10.5194/hess-18-
 532 953-2014
- 533 Boorman, L., & Fuller, R. (1981). The changing status of reedswamp in the Norfolk Broads. *Journal of Applied*
 534 *Ecology*, 18(1), 241-269. doi:10.2307/2402493.
- 535 Bubier, J. L., Moore, T. R., & Roulet, N. T. (1993). Methane Emissions from Wetlands in the Midboreal Region
 536 of Northern Ontario, Canada. *Ecology*, 74(8), 2240-2254. doi:10.2307/1939577
- 537 Cadillo-Quiroz, H., Yashiro, E., Yavitt, J., & Zinder, S. (2008). Characterization of the archaeal community in a
 538 minerotrophic fen and terminal restriction fragment length polymorphism-directed isolation of a novel
 539 hydrogenotrophic methanogen. *Applied and Environmental Microbiology*, 74(7), 2059-2068.
 540 doi:10.1128/AEM.02222-07|10.1128/AEM.02222-07

- 541 Chanton, J. P. (2005). The effect of gas transport on the isotope signature of methane in wetlands. *Organic*
542 *Geochemistry*, 36(5), 753-768. doi:10.1016/j.orggeochem.2004.10.007
- 543 Chen, X., & Slater, L. (2015). Gas bubble transport and emissions for shallow peat from a northern peatland:
544 The role of pressure changes and peat structure. *Water Resources Research*, 51(1), 151-168.
545 doi:10.1002/2014WR016268
- 546 Christensen, T. R., Panikov, N., Mastepanov, M., Joabsson, A., Stewart, A., Öquist, M., Sommerkorn, M.,
547 Reynaud, S., & Svensson, B. (2003). Biotic controls on CO₂ and CH₄ exchange in wetlands – a closed
548 environment study. *Biogeochemistry*, 64(3), 337-354. doi:10.1023/a:1024913730848
- 549 Clever, H. L., & Young, C. L. (Eds.). (1987). *Solubility Data Series. Vol. 27–28. Methane.* : International Union
550 of Pure and Applied Chemistry. URL: <https://srdata.nist.gov/solubility/IUPAC/SDS-27-28/SDS-27-28.aspx>.
- 551 Comas, X., & Wright, W. (2012). Heterogeneity of biogenic gas ebullition in subtropical peat soils is revealed
552 using time-lapse cameras. *Water Resources Research*, 48(4). doi:10.1029/2011WR011654
- 553 Coulthard, T. J., Baird, A. J., Ramirez, J., & Waddington, J. M. (2009). Methane dynamics in peat: Importance
554 of shallow peats and a novel reduced-complexity approach for modeling ebullition. In A. J. Baird, L. R. Belyea,
555 X. Comas, & L. D. Slater (Eds.), *Carbon Cycling in Northern Peatlands* (pp. 173-185). Washington, DC:
556 American Geophysical Union.
- 557 Denmead, O. T. (2008). Approaches to measuring fluxes of methane and nitrous oxide between landscapes and
558 the atmosphere. *Plant and Soil*, 309(1-2), 5-24. doi:10.1007/s11104-008-9599-z
- 559 Dunfield, P., Knowles, R., Dumont, R., & Moore, T. R. (1993). Methane production and consumption in
560 temperate and subarctic peat soils: Response to temperature and pH. *Soil Biology and Biochemistry*, 25(3), 321-
561 326. doi:10.1016/0038-0717(93)90130-4
- 562 Fechner-Levy, E. J., & Hemond, H. F. (1996). Trapped methane volume and potential effects on methane
563 ebullition in a northern peatland. *Limnology and Oceanography*, 41(7), 1375-1383.
564 doi:10.4319/lo.1996.41.7.1375
- 565 Flury, S., McGinnis, D. F., & Gessner, M. O. (2010). Methane emissions from a freshwater marsh in response to
566 experimentally simulated global warming and nitrogen enrichment. *Journal of Geophysical Research:*
567 *Biogeosciences*, 115(G1), n/a-n/a. doi:10.1029/2009JG001079
- 568 Frenzel, P., & Rudolph, J. (1998). Methane emission from a wetland plant: the role of CH₄ oxidation in
569 *Eriophorum*. *Plant and Soil*, 202(1), 27-32. doi:10.1023/a:1004348929219
- 570 Frolking, S., & Roulet, N. T. (2007). Holocene radiative forcing impact of northern peatland carbon
571 accumulation and methane emissions. *Global Change Biology*, 13(5), 1079-1088. doi:10.1111/j.1365-
572 2486.2007.01339.x
- 573 Glaser, P., Chanton, J., Morin, P., Rosenberry, D., Siegel, D., Ruud, O., Chasar, L., & Reeve, A. (2004). Surface
574 deformations as indicators of deep ebullition fluxes in a large northern peatland. *Global Biogeochemical Cycles*,
575 18(1). doi:10.1029/2003GB002069
- 576 Goodrich, J. P., Varner, R. K., Frolking, S., Duncan, B. N., & Crill, P. M. (2011). High-frequency measurements
577 of methane ebullition over a growing season at a temperate peatland site. *Geophysical Research Letters*, 38(7),
578 doi: 10.1029/2011GL046915
- 579 Green, S. M., & Baird, A. J. (2012). A mesocosm study of the role of the sedge *Eriophorum angustifolium* in the
580 efflux of methane—including that due to episodic ebullition—from peatlands. *Plant and Soil*, 351(1-2), 207-
581 218. doi:10.1007/s11104-011-0945-1
- 582 Green, S. M., & Baird, A. J. (2013). The importance of episodic ebullition methane losses from three peatland
583 microhabitats: a controlled-environment study. *European Journal of Soil Science*, 64(1), 27-36.
584 doi:10.1111/ejss.12015
- 585 Gumbrecht, T., Roman-Cuesta, R. M., Verchot, L., Herold, M., Wittmann, F., Householder, E., Herold, N., &
586 Murdiyarto, D. (2017). An expert system model for mapping tropical wetlands and peatlands reveals South
587 America as the largest contributor. *Global Change Biology*, 23(9), 3581-3599. doi:10.1111/gcb.13689
- 588 Hendriks, D. M. D., van Huissteden, J., Dolman, A. J., & van der Molen, M. K. (2007). The full greenhouse gas
589 balance of an abandoned peat meadow. *Biogeosciences*, 4(3), 411-424. doi:10.5194/bg-4-411-2007
- 590 Heppell, C. M.; Stanley, K.M.; Belyea, L.R. (2018). Methane ebullition from two lowland floodplain fens.
591 NERC Environmental Information Data Centre. [https://doi.org/10.5285/8d42ea20-6e8f-4b39-a735-
592 8a6b3b95984e](https://doi.org/10.5285/8d42ea20-6e8f-4b39-a735-8a6b3b95984e)
- 593 Hoffmann, M., Schulz-Hanke, M., Garcia Alba, J., Jurisch, N., Hagemann, U., Sachs, T., Sommer, M., &
594 Augustin, J. (2017). A simple calculation algorithm to separate high-resolution CH₄ flux measurements into
595 ebullition- and diffusion-derived components. *Atmospheric Measurement Techniques*, 10(1), 109-118.
596 doi:10.5194/amt-10-109-2017
- 597 Hornibrook, E. R. C., Bowes, H. L., Culbert, A., & Gallego-Sala, A. V. (2009). Methanotrophy potential versus
598 methane supply by pore water diffusion in peatlands. *Biogeosciences*, 6(8), 1490-1504. doi:10.5194/bg-6-1491-
599 2009
- 600 IUCN. (2017). *Phragmites australis*. Retrieved from <http://www.iucnredlist.org/details/164494/0> Accessed
601 18/10/2017
- 602 Joabsson, A., & Christensen, T. R. (2001). Methane emissions from wetlands and their relationship with
603 vascular plants: an Arctic example. *Global Change Biology*, 7(8). doi:10.1046/j.1354-1013.2001.00044.x

- 604 Kellner, E., Baird, A., Oosterwoud, M., Harrison, K., & Waddington, J. (2006). Effect of temperature and
605 atmospheric pressure on methane (CH₄) ebullition from near-surface peats. *Geophysical Research Letters*,
606 33(18), L18405. doi:10.1029/2006GL027509
- 607 Kettridge, N., & Binley, A. (2008). X-ray computed tomography of peat soils: measuring gas content and peat
608 structure. *Hydrological Processes*, 22(25), 4827-4837. doi:10.1002/hyp.7097
- 609 Kotsyurbenko, O.R., Chin, K.J., Glagolev, M. V., Stubner, S., Simankova, M. V., Nozhevnikova,
610 A.N., and Conrad, R. (2004) Acetoclastic and hydrogenotrophic methane production and
611 methanogenic populations in an acidic West-Siberian peat bog. *Environ. Microbiol.* 6:
612 1159-1173, doi:10.1111/j.1462-2920.2004.00634.x.
- 613 Laanbroek, H. J. (2010). Methane emission from natural wetlands: interplay between emergent macrophytes and
614 soil microbial processes. A mini-review. *Annals of Botany*, 105(1), 141-153. doi:10.1093/aob/mcp201
- 615 Limpens, J., Berendse, F., Blodau, C., Canadell, J., Freeman, C., Holden, J., Roulet, N., Rydin, H., &
616 Schaeppman-Strub, G. (2008). Peatlands and the carbon cycle: from local processes to global implications - a
617 synthesis. *Biogeosciences*, 5(5), 1475-1491. doi:10.5194/bg-5-1475-2008.
- 618 Maltby, E., Ormerod, S., Acreman, M., Dunbar, M., Jenkins, A., Maberly, S., Newman, J., Blackwell,
619 M., Ward, R. (2011) Chapter 9. Freshwaters : openwaters, wetlands and floodplains In: *UK National Ecosystem*
620 *Assessment: understanding nature's value to society. Technical Report.* Cambridge, UK, UNEP-WCMC, 295-
621 360.
- 622 Noyce, G. L., Varner, R. K., Bubier, J. L., & Frohling, S. (2014). Effect of *Carex rostrata* on seasonal and
623 interannual variability in peatland methane emissions. *Journal of Geophysical Research: Biogeosciences*,
624 119(1), 24–34, doi:10.1002/2013JG002474.
- 625 Olde Venterink, H., van der Vliet, R. E., & Wassen, M. J. (2001). Nutrient limitation along a productivity
626 gradient in wet meadows. *Plant and Soil*, 234(2), 171-179, doi: 10.1023/A:1017922715903.
- 627 Petrescu, A. M. R., Lohila, A., Tuovinen, J.-P., Baldocchi, D. D., Desai, A. R., Roulet, N. T., Vesala, T.,
628 Dolman, A. J., Oechel, W. C., Marcolla, B., Friborg, T., Rinne, J., Matthes, J. H., Merbold, L., Meijide, A.,
629 Kiely, G., Sottocornola, M., Sachs, T., Zona, D., Varlagin, A., Lai, D. Y. F., Veenendaal, E., Parmentier, F.-J.
630 W., Skiba, U., Lund, M., Hensen, A., van Huissteden, J., Flanagan, L. B., Shurpali, N. J., Grünwald, T.,
631 Humphreys, E. R., Jackowicz-Korczyński, M., Aurela, M. A., Laurila, T., Grüning, C., Corradi, C. A. R.,
632 Schrier-Uijl, A. P., Christensen, T. R., Tamstorf, M. P., Mastepanov, M., Martikainen, P. J., Verma, S. B.,
633 Bernhofer, C., & Cescatti, A. (2015). The uncertain climate footprint of wetlands under human pressure.
634 *Proceedings of the National Academy of Sciences*, 112(15), 4594-4599. doi:10.1073/pnas.1416267112
- 635 Ramirez, J. A., Baird, A. J., & Coulthard, T. J. (2017). The effect of sampling effort on estimates of methane
636 ebullition from peat. *Water Resources Research*, 53(5), 4158-4168. doi:10.1002/2017WR020428
- 637 Shannon, R. D., White, J. R., Lawson, J. E., & Gilmour, B. S. (1996). Methane Efflux from Emergent
638 Vegetation in Peatlands. *Journal of Ecology*, 84(2), 239-246. doi:10.2307/2261359
- 639 Shotyk, W. (1988). Review of the inorganic geochemistry of peats and peatland waters. *Earth-Science Reviews*,
640 25(2), 95-176. doi:10.1016/0012-8252(88)90067-0
- 641 Smirnov, B. M., & Berry, R. S. (2015). Growth of bubbles in liquid. *Chemistry Central Journal*, 9(1), 48.
642 doi:10.1186/s13065-015-0127-y
- 643 Stamp, I., Baird, A. J., & Heppell, C. M. (2013). The importance of ebullition as a mechanism of methane
644 (CH₄) loss to the atmosphere in a northern peatland. *Geophysical Research Letters*, 40(10), 2087–2090.
645 doi:10.1002/grl.50501
- 646 Strack, M., Kellner, E., & Waddington, J. M. (2005). Dynamics of biogenic gas bubbles in peat and their effects
647 on peatland biogeochemistry. *Global Biogeochemical Cycles*, 19(1). doi:10.1029/2004GB002330
- 648 Strack, M., Mwakanyamale, K., Hassanpour Fard, G., Bird, M., Berube, V., Rochefort, L. (2017). Effect of
649 plant functional type on methane dynamics in a restored minerotrophic peatland. *Plant and Soil*, 410, 231-246,
650 doi: 10.1007/s11104-016-2999-6.
- 651 Syed, K. H., Flanagan, L. B., Carlson, P. J., Glenn, A. J., & Van Gaalen, K. E. (2006). Environmental control of
652 net ecosystem CO₂ exchange in a treed, moderately rich fen in northern Alberta. *Agricultural and Forest*
653 *Meteorology*, 140(1), 97-114, doi: 10.1016/j.agrformet.2006.03.022.
- 654 Tokida, T., Miyazaki, T., Mizoguchi, M., & Seki, K. (2005). In situ accumulation of methane bubbles in a
655 natural wetland soil. *European Journal of Soil Science*, 56(3), 389-396. doi:10.1111/j.1365-2389.2004.00674.x
- 656 Troels-Smith, J. (1955). *Karakterisering af løse jordarter. Characterization of unconsolidated sediments.*
657 Copenhagen: C.A. Reitzel.
- 658 Turetsky, M. R., Kotowska, A., Bubier, J., Dise, N. B., Crill, P., Hornibrook, E. R. C., Minkinen, K., Moore, T.
659 R., Myers-Smith, I. H., Nykänen, H., Olefeldt, D., Rinne, J., Saarnio, S., Shurpali, N., Tuittila, E.-S.,
660 Waddington, J. M., White, J. R., Wickland, K. P., & Wilking, M. (2014). A synthesis of methane emissions
661 from 71 northern, temperate, and subtropical wetlands. *Global Change Biology*, 20(7), 2183-2197.
662 doi:10.1111/gcb.12580
- 663 UK Biodiversity Action Plan. (2008). *Priority Habitat Descriptions, BRIG.* Retrieved from Joint Nature
664 Conservation Committee: <http://jncc.defra.gov.uk/page-5706> Accessed online on 20/09/2017

- 665 van den Berg, M., Ingwersen, J., Lamers, M., & Streck, T. (2016). The role of Phragmites in the CH₄ and CO₂
666 fluxes in a minerotrophic peatland in southwest Germany. *Biogeosciences*, 13(21), 6107-6119. doi:10.5194/bg-
667 13-6107-2016
- 668 van Winden, J. F., Reichart, G.-J., McNamara, N. P., Benthien, A., & Damsté, J. S. S. (2012). Temperature-
669 Induced Increase in Methane Release from Peat Bogs: A Mesocosm Experiment. *PLOS ONE*, 7(6), e39614.
670 doi:10.1371/journal.pone.0039614
- 671 Wassen, M. J., & Olde Venterink, H. (2006). Comparison of nitrogen and phosphorus fluxes in some European
672 fens and floodplains. *Applied Vegetation Science*, 9(2), 213-222, doi: 10.1111/j.1654-109X.2006.tb00670.x.
- 673 Wilson, D., Alm, J., Riutta, T., Laine, J., Byrne, K., Farrell, E., & Tuittila, E.-S. (2007). A high resolution green
674 area index for modelling the seasonal dynamics of CO₂ exchange in peatland vascular plant communities. *Plant*
675 *Ecology*, 190(1), 37-51. doi:10.1007/s11258-006-9189-1
- 676 Wood, S., & Scheipl, F. (2017). gamm4: Generalized Additive Mixed Models using 'mgcv' and 'lme4'. R
677 package version 0.2-5. Vienna, Austria: R Foundation for Statistical Computing. Retrieved from [https://cran.r-](https://cran.r-project.org/package=gamm4)
678 [project.org/package=gamm4](https://cran.r-project.org/package=gamm4)
- 679 Yamamoto, S., Alcauskas, J. B., & Crozier, T. E. (1976). Solubility of methane in distilled water and seawater.
680 *Journal of Chemical and Engineering Data*, 21(1), 78-80, doi: 10.1021/je60068a029.
- 681 Yu, Z., Slater, L. D., Schäfer, K. V., Reeve, A. S., & Varner, R. K. (2014). Dynamics of methane ebullition
682 from a peat monolith revealed from a dynamic flux chamber system. *Journal of Geophysical Research:*
683 *Biogeosciences*, 119(9), 1789-1806. doi:10.1002/2014JG002654
- 684
- 685
- 686

687 **Tables**

688

689 Table 1. Site vegetation and nutrient status.

Site	NB-HN ^a	NB-LN ^a
Dominant plant species	<i>P. australis</i> , <i>Eupatorium</i> <i>cannabinum</i> L. (1753)	<i>P. australis</i> , <i>Peucedanum palustre</i> (L.) Moench (1794)
Mean aboveground biomass (g m⁻²)^b	1578 (169, n=6)	435 (42, n=6)
Plant height (cm)^b	107 (7.8, n=6)	57 (5.1, n=6)
Foliar N content (g kg⁻¹)^b	22 (1.5, n=6)	16 (1.5, n=6)
Foliar P content (g kg⁻¹)^b	2 (0.2, n=6)	1.1 (0.1, n=6)
Foliar C/N quotient^b	20 (1.4, n=6)	27 (2.8, n=6)
Foliar C/P quotient^b	210 (2.3, n=6)	388 (5.2, n=6)
Foliar N/P quotient^b	11 (0.9, n=6)	15 (1.3, n=6)
Peat depth (m)^c	9.0	5.0
Peat N content (g kg⁻¹, 0-15 cm depth)^d	28 (0.4, n=5)	18 (0.9, n=5)
Peat P content (g kg⁻¹, 0-15 cm depth)^d	0.9 (0.02, n=5)	0.4 (0.01, n=5)
Peat C/N quotient (0-15 cm depth)^d	13 (0.22, n=5)	20 (0.5, n=5)
Peat C/P quotient (0-15 cm depth)^d	502 (23, n=5)	856 (62, n=5)
Peat N/P quotient (0-15 cm depth)^d	31 (1.1, n=5)	45 (2.5, n=5)
Peat pH	6.5 (0.01, n = 3)	6.5 (0.02, n = 3)
Peat electrical conductivity (μS cm⁻¹)^d	863 (83, n = 3)	1715 (169, n = 3)

690 ^aData in brackets are ±1 Standard Error of *n* replicates per site. ^bSampled in Sept 2012.691 ^cLambert et al. (1960). ^dSampled in March 2013.

692

693

694

695

696

697

698

699

700

701

702 Table 2. Goodness-of-fit information for time-series GAMM models of bubble volume flux,
 703 methane concentration, methane ebullition flux (all from funnels) and methane flux from
 704 static chambers. Results are shown for models including increasing numbers of random
 705 (funnel or chamber) and fixed (constant, Site, DOY, where DOY is day of year) effects. The
 706 final model described in the main text is shown in italic font. Smooth functions are denoted
 707 by $s(\dots)$. The number of parameters used in the model is given by df. ΔAICc is the corrected
 708 Akaike Information Criterion (AICc) of the model of interest, minus the AICc of the final
 709 model. Deviance, a goodness-of-fit statistic used when the statistical model is fit by
 710 maximum-likelihood, measures the deviation from a model that is a perfect fit to the data. D^2
 711 is the percentage deviance explained by the model of interest, referenced to the null model.
 712

Model formula	Note	df	ΔAICc	Deviance	D^2 (%)
Bubble volume flux ~					
constant	null	2.0	104	407	-
constant + s(funnel)	random only	20.9	111	311	24
constant + s(funnel) + Site		19.1	103	306	25
constant + s(funnel) + s(DOY)		16.6	2	156	62
<i>constant + s(funnel) + Site + s(DOY)</i>	<i>final</i>	<i>17.1</i>	<i>0</i>	<i>153</i>	<i>62</i>
Methane concentration ~					
constant	null	2.0	117	492	-
constant + s(funnel)	random only	20.3	125	387	21
constant + s(funnel) + Site		16.1	115	393	20
constant + s(funnel) + s(DOY)		23.8	7	157	68
<i>constant + s(funnel) + Site + s(DOY)</i>	<i>final</i>	<i>21.3</i>	<i>0</i>	<i>158</i>	<i>68</i>
Methane ebullition flux ~					
constant	null	2.0	164	707	-
constant + s(funnel)	random only	11.6	174	657	7
constant + s(funnel) + Site		8.0	168	669	5
constant + s(funnel) + s(DOY)		17.6	3	193	73
<i>constant + s(funnel) + Site + s(DOY)</i>	<i>final</i>	<i>17.9</i>	<i>0</i>	<i>188</i>	<i>73</i>
Chamber methane flux ~					
constant	null	2.0	41	118	-
constant + s(chamber)	random only	10.5	20	66	44
constant + s(chamber) + Site		11.0	21	65	44
constant + s(chamber) + s(DOY)		14.2	-1	40	66
<i>constant + s(chamber) + Site + s(DOY)</i>	<i>final</i>	<i>14.7</i>	<i>0</i>	<i>40</i>	<i>66</i>

713

714

715

716 Table 3. Goodness-of-fit information for controlling-factors GAMM models of bubble
 717 volume flux, methane concentration and methane ebullition flux. Results are shown for

718 models including increasing numbers of random (funnel) and fixed effects. The final model
 719 presented in the main text is shown in italic font. Smooth functions are denoted by $s(\dots)$. The
 720 number of parameters used in the model is given by df. ΔAICc is the corrected Akaike
 721 Information Criterion (AICc) of the model of interest, minus the AICc of the final model.
 722 Deviance, a goodness-of-fit statistic used when the statistical model is fit by maximum-
 723 likelihood, measures the deviation from a model that is a perfect fit to the data. D^2 is the
 724 percentage deviance explained by the model of interest, referenced to the null model. Fixed
 725 effects are abbreviated as follows: MST, mean soil temperature ($^{\circ}\text{C}$); SDAP, standard
 726 deviation of air pressure (cm water); MWL, mean water level (cm); VGA, vascular green
 727 area (unitless); SLAP, slope of air pressure (cm water h^{-1}).
 728

Model formula	Note	df	ΔAICc	Deviance	D^2 (%)
Bubble volume flux ~					
constant	null	2.0	115	407	-
constant + s(funnel)	random only	20.9	122	311	24
constant + s(funnel) + s(SDAP)		19.5	18	154	62
constant + s(funnel) + s(MST)		18.3	7	145	64
<i>constant + s(funnel) + s(MST) + s(SDAP)</i>	<i>final</i>	<i>17.9</i>	<i>0</i>	<i>139</i>	<i>66</i>
Methane concentration ~					
constant	null	2.0	129	492	-
constant + s(funnel)	random only	20.3	137	387	21
constant + s(funnel) + s(VGA)		27.1	16	142	71
constant + s(funnel) + s(MST)		30.1	6	121	76
constant + s(funnel) + s(MWL)		26.4	1	129	74
<i>constant + s(funnel) + s(MST) + s(MWL)</i> <i>+ s(VGA)</i>	<i>final</i>	<i>25.9</i>	<i>0</i>	<i>129</i>	<i>74</i>
Methane ebullition flux ~					
constant	null	2.0	172	707	-
constant + s(funnel)	random only	11.6	179	657	7
constant + s(funnel) + s(SLAP)		6.1	162	634	10
constant + s(funnel) + s(MWL)		17.4	17	212	70
constant + s(funnel) + s(MST)		28.3	6	166	77
constant + s(funnel) + s(VGA)		21.3	3	181	75
<i>constant + s(funnel) + s(MST) + s(MWL)</i> <i>+ s(VGA) + s(SLAP)</i>	<i>final</i>	<i>16.5</i>	<i>0</i>	<i>190</i>	<i>73</i>

729
 730
 731
 732
 733
 734
 735
 736

737

738 **Figure 1.** Location map of Sutton (NB-LN) and Strumpshaw (NB-HN) Fen. For full
739 description of peat horizons see Table S2.

740

741 **Figure 2.** Time series of a) bubble volume flux, b) methane concentration and c) methane
742 ebullition flux from the funnels, and d) methane flux from the chambers. Lines and shading
743 are summed effects (mean \pm 95% confidence intervals) of the generalized additive mixed
744 models, with day of year as a smooth term, site as a fixed factor on the intercept and funnel as
745 a random effect on the intercept.

746

747 **Figure 3.** Conditional effects (\pm 95% confidence intervals) of environmental variables on
748 bubble volume flux (top row), methane concentration (middle row) and methane ebullition
749 flux (bottom row). Funnel was included as a random effect on the intercept.

750

751 **Figure 4.** Separation of total CH₄ fluxes into contributions from different transport
752 mechanisms. a) CH₄ fluxes (median \pm interquartile range, summed from days 102 to 211)
753 determined by chamber and funnel methods. The line within the bar for NB-LN funnel
754 method is the flux for a period of high water levels, i.e., the peatland was either flooded or
755 water level was less than 5 cm below the peatland surface (days 102 to 168; see also Fig.
756 S1b). For NB-HN, the summed funnel flux for the period of high water levels (days 102 to
757 187) was indistinguishable from that for the full period. b) Time series of total CH₄ fluxes
758 with contributions from different transport mechanisms, presented by site (columns) and
759 idealized extreme model (rows). Each panel shows a time series of estimated fluxes due to
760 diffusion + plant-mediated transport, stacked on to steady + episodic ebullition. Total flux is
761 shown as a black line. The idealized extreme models were as follows. Upper panels: If steady
762 ebullition is zero, the funnel captures episodic ebullition only and total emission is equal to
763 the sum of chamber and funnel fluxes. Lower panels: If episodic ebullition is zero, the funnel
764 captures steady ebullition only and total emission is equal to chamber flux only. Under the
765 latter extreme, the negative contribution by diffusion + plant-mediated transport in mid-
766 season indicates either that CH₄ was taken up from the atmosphere or, more likely, that the
767 idealized model of zero episodic emission was invalid. Both extreme models assume that
768 bubbles collected by the funnels at 40 cm depth would have been transported to the peatland
769 surface without oxidation. This assumption is likely to have been met during the period of
770 high water levels, shown to the left of the dashed grey line (day 102 to 187 for NB-HN and
771 day 102 to 168 for NB-LN). Bubble production in the 40-cm thick zone above the funnel is
772 not included in the estimates of ebullition flux.

773

774

775

776

Figure 1.

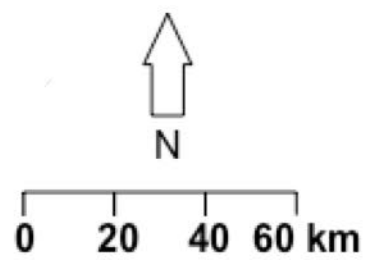
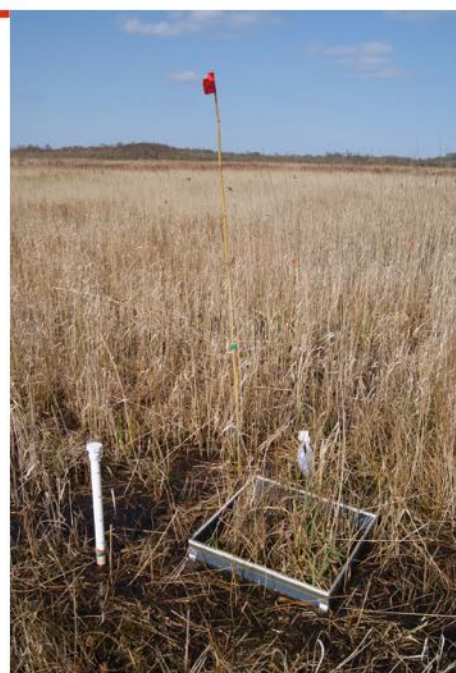


Figure 2.

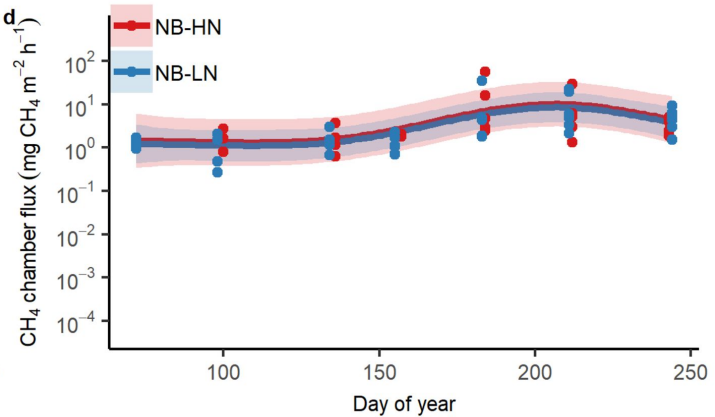
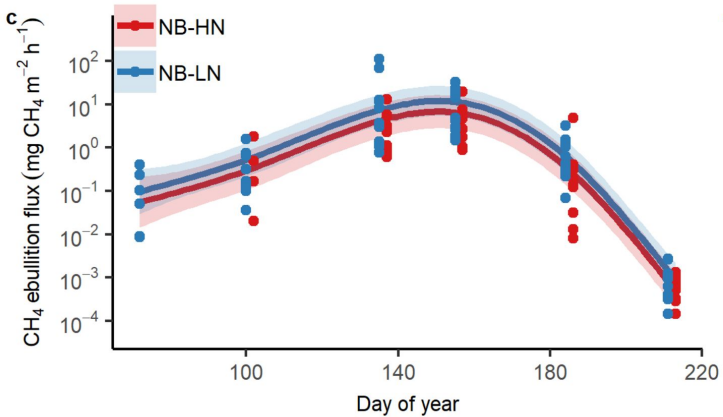
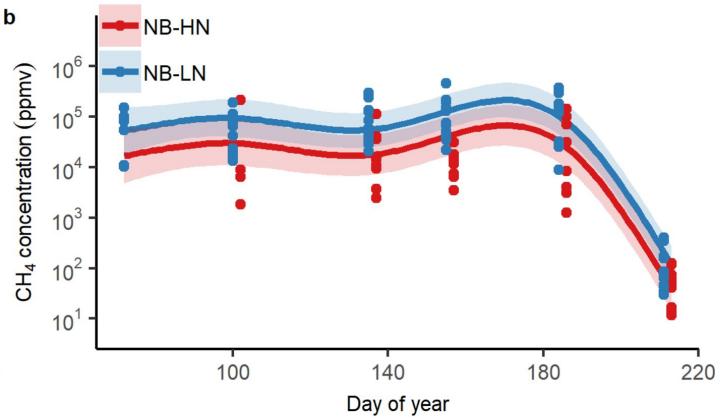
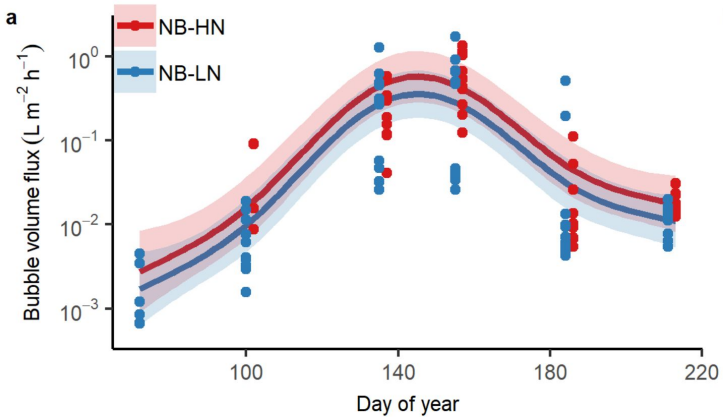


Figure 3.

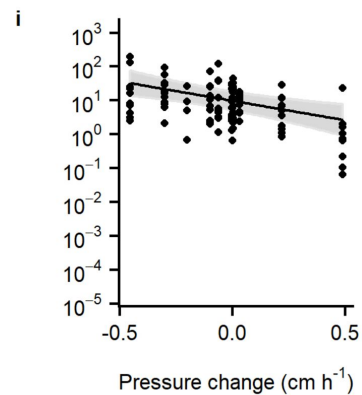
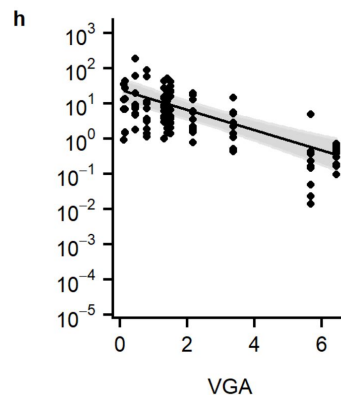
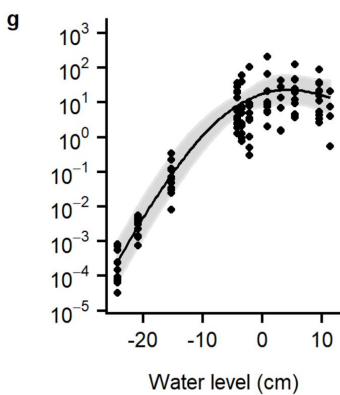
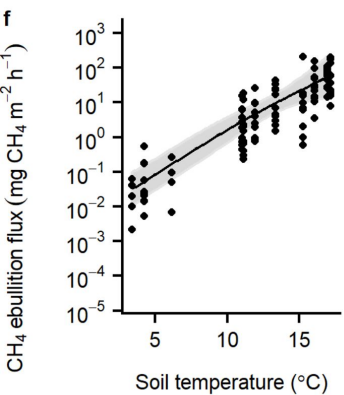
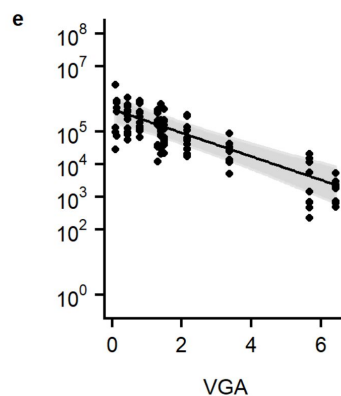
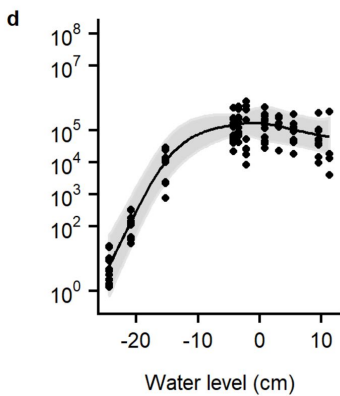
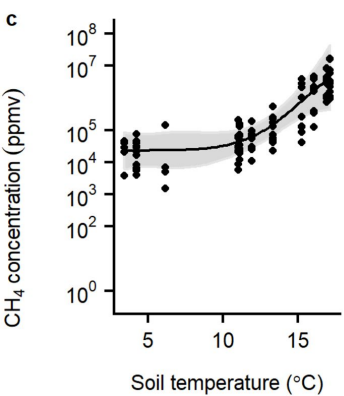
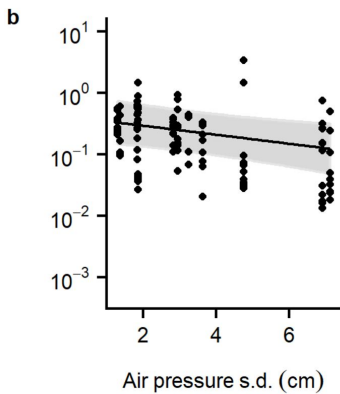
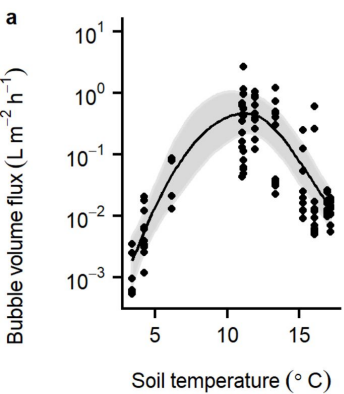


Figure 4.

